Electronic Supplementary Information (ESI)

Oxidatively Stable Fluorinated Sulfone Electrolytes for High Voltage High Energy Lithium-ion Battery

Chi-Cheung Su,[a] Meinan He,[a] Paul C. Redfern,[b] Larry A. Curtiss,[b] Ilya A. Shkrob[a] and Zhengcheng Zhang[*a]

*[a]Chemical Sciences and Engineering Division*

[b]Materials Science Division

Argonne National Laboratory, 9700 S. Cass Av., Argonne, IL 60439, USA

E-mail: zzhang@anl.gov; 1-630-252-7868
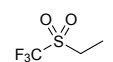
S1. Synthesis of Fluorinated Sulfones

Our general synthetic strategy is illustrated in Scheme S1. Scheme S1a shows the synthetic route for FMES and FMPS. Both sulfones were synthesized by reacting trifluoromethanesulfonic anhydride (TFMSA) with dialkylmagnesium, which was prepared in a reaction of alkyl magnesium bromide with 1,4-dioxane. The use of dialkylmagnesium instead of alkyl magnesium bromide was due to oxidation of the bromide ion in alkyl magnesium bromide by TFMSA. Although TFMSA cannot oxidize alkyl magnesium chloride, this reaction results in a significant amount of dialkyl sulfide byproduct which not only decreased the product yield, but also complicated purification of the product. In contrast, FMIS can be prepared by reacting TFMSA directly with isopropyl magnesium chloride in diethyl ether, as shown in Scheme S1b. The steric hindrance of the isopropyl group suppresses the formation of dialkyl byproducts, and thus FMIS can be synthesized in a one-step reaction. Scheme S1c shows the unique synthesis route for FPMS, the previous reported fluorosulfone. The nucleophilic reaction between bis(3,3,3-trifluoropropyl)magnesium (synthesized in a reaction of (3,3,3-trifluoropropyl)magnesium iodide with 1,4-dioxane) and methanesulfonic anhydride generates FPMS with decent yield.
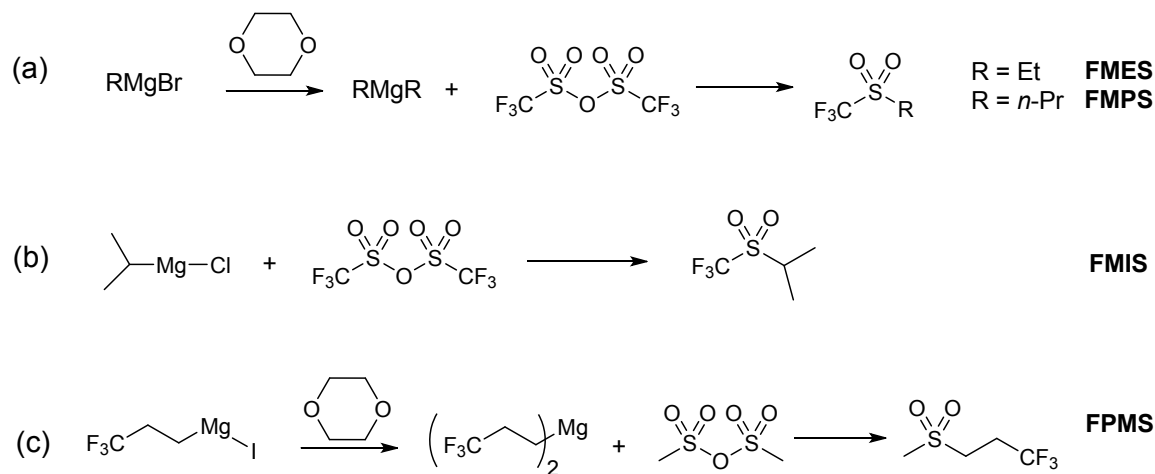
Scheme S1. Synthetic routes for fluorinated sulfone FMES, FMPS, FMIS and FPMS.

All newly reported synthetic organic molecules were characterized by NMR spectroscopy and gas chromatography – mass spectrometry (GC-MS) to confirm the structure and purity. ^{1}H, ^{13}C and ^{19}F NMR spectra of these compounds are shown in Figs. S1 to S12. NMR spectra were obtained using an Avance DMX 500 MHz Bruker spectrometer. ^{1}H and ^{13}C chemical shifts in parts per million (ppm) are referenced to tetramethylsilane. For GC-MS measurements, 1 µL liquid sample was loaded in a splitless mode on an HP-5MS (bore 0.25 µm, length 30 m) column using an Agilent Technologies Model 7890B chromatograph equipped with a Model 5977 mass detector.

S1.1 Trifluoromethyl ethyl suflone (FMES)

To a solution of ethylmagnesium bromide (118.9 mL, 0.357 mol) in 200 mL anhydrous diethyl ether (3.0 M) was added dropwise anhydrous 1,4-dioxane (31.4 g, 0.357 mol) at 0 ºC. The mixture was centrifuged at 3,000 rpm until the solid residue separated. The supernatant was then added dropwise using a syringe pump to a solution of trifluoromethanesulfonic anhydride (67.1 g, 0.238 mol) in 200 mL

anhydrous diethyl ether at -78 °C. The reaction mixture was stirred at -78 °C for 20 min and then quenched by adding 50 mL 0.5 N aqueous hydrochloric acid. The organic phase was separated, and the aqueous phase was further extracted with 3X 50 mL diethyl ether. The combined organic phase was washed with brine and dried over anhydrous Na_2SO_4. After the removal of solvent in vacuum, the crude product was dried over 4 Å molecular sieves and purified by fractional distillation. The final product (b.p. 141°C) is a colourless liquid (15.1 g, 93.1 mmol) obtained with a yield of 39%.

^{1}H NMR (CDCl$_3$, 500 MHz): δ 3.29 (q, 2H, J=7.6 Hz), 1.52 (t, 3H, J=7.6 Hz); ^{13}C NMR (CDCl$_3$, 125 MHz): δ 123.4, 120.8, 118.2, 115.6 (q, J=325 Hz), 44.5, 5.5; MS-EI *m/z*: 163.0 [M+H]$^+$: 146.0, 93.0, 77.0, 69.0, 65.0.

S1.2 Trifluoromethyl propyl sulfone (FMPS)
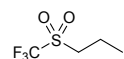
To a suspension of magnesium powder (11.2 g, 0.461 mol) in 150 mL anhydrous diethyl ether was added dropwise 1-bromopropane (47.1 g, 0.383 mol) using a syringe pump at room temperature. This reaction was carried out in an oven-dried flask equipped with a condenser and purged with dry nitrogen. The reaction mixture was stirred at room temperature for 1 h before the supernatant was transferred to a clean, oven-dried centrifuge tube. Anhydrous 1,4-dioxane (33.7 g, 0.383 mol) was then added at 0 °C and the suspension was centrifuged until the solid residue separated. The supernatant was added dropwise using a syringe pump to a solution of trifluoromethanesulfonic anhydride (60.0 g, 0.213 mol) in 200 mL anhydrous diethyl ether at -78 °C. The subsequent treatment followed the procedure outlined in section S1.1. The final product (b.p. 152 °C) is a colourless liquid (16.5 g, 0.0937 mol) obtained with a yield of 44%.

^{1}H NMR (CDCl$_3$, 500 MHz): δ 3.20 (t, 2H, J=7.8 Hz), 1.96 (dt, 2H, J=7.8 Hz, J=7.7 Hz), 1.13 (t, 3H, J=7.5 Hz); ^{13}C NMR (CDCl$_3$, 125 MHz): δ 123.3, 120.7, 118.1, 115.5 (q, J=325 Hz), 51.1, 14.7, 12.8; MS-EI *m/z*: 177.0 [M+H]$^+$: 148.0, 135.0, 107.0, 79.0, 69.0, 63.0.

S1.3 Trifluoromethyl isopropyl sulfone (FMIS)
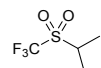
Isopropylmagnesium chloride solution (106 mL, 0.212 mol) in diethyl ether (2.0 M) was added dropwise unsing a syringe pump to a solution of trifluoromethanesulfonic anhydride (50.0 g, 0.177 mol) in 150 mL anhydrous diethyl ether at -78 °C. The reaction mixture was stirred at -78 °C for 40 min and quenched by adding 40 mL 0.5 N aqueous HCl. The subsequent treatment followed the procedure given in section S1.1. The final product (b.p.:150 °C) is a colourless liquid (10.1 g, 0.0573 mol) obtained with a yield of 32%.

^{1}H NMR (CDCl$_3$, 500 MHz): δ 3.49 (septet, 1H, J=6.9 Hz), 1.48 (dq, 6H, J=7.0 Hz, J=0.9 Hz); ^{13}C NMR (CDCl$_3$, 125 MHz): δ 123.8, 121.2, 118.6, 116.0 (q, J=327 Hz), 52.5, 14.7; MS-EI *m/z*: 177.0 [M + H]$^+$: 135.0, 107.0, 91.1, 69.0, 62.0.

S1.4 Trifluoropropyl methyl sulfone (FPMS)
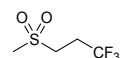
To a suspension of magnesium powder (6.62 g, 0.272 mol) in 150 mL anhydrous diethyl ether in an oven-dried flask under nitrogen was added dropwise 1,1,1-trifluoro-3-iodopropane (50.9 g, 0.227 mol) via a syringe pump at room temperature. The reaction mixture was stirred at room temperature for 1 h before the supernatant was transferred to a clean, oven-dried centrifuge tube. Anhydrous 1,4-dioxane (20.0

3

g, 0.227 mol) was then added at 0 °C and the suspension was centrifuged until the solid residue separated. The supernatant was then added dropwise using a syringe pump to a solution of trifluoromethanesulfonic anhydride (40.0 g, 0.142 mol) in 150 mL anhydrous diethyl ether at -78 °C. The reaction mixture was stirred at -78 °C for 20 min and was then quenched by adding 50 mL 0.5 N aqueous HCl. The subsequent treatment followed the procedure given in section S1.1. The crude product was purified by vacuum sublimation. The final product is a white powder (9.26 g, 0.0526 mol) obtained with a yield of 37%.

^{1}H NMR (CDCl$_3$, 500 MHz): δ 3.24 (m, 2H, 6.9 Hz), 2.98 (s, 3H), 2.66 (dt, 2H, J=7.0 Hz, J=7.1 Hz); ^{13}C NMR (CDCl$_3$, 125 MHz): δ 128.7, 126.5, 124.3, 122.1 (q, J=275 Hz), 47.6, 47.5, 47.5, 47.5 (q, J=2.7 Hz), 27.5, 27.3, 27.0, 26.8 (q, 31.5 Hz); MS-EI m/z: 176.0 [M]$^+$: 161.0, 107.0, 97.0, 77.1, 65.0, 51.0.
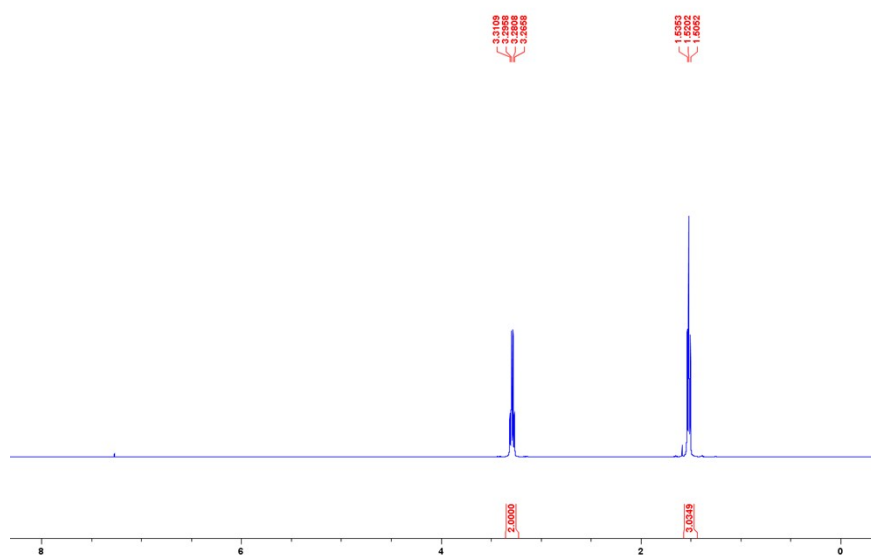

Fig. S1 ^{1}H NMR spectrum of ((trifluoromethyl)sulfonyl)ethane (FMES) in CDCl$_3$.
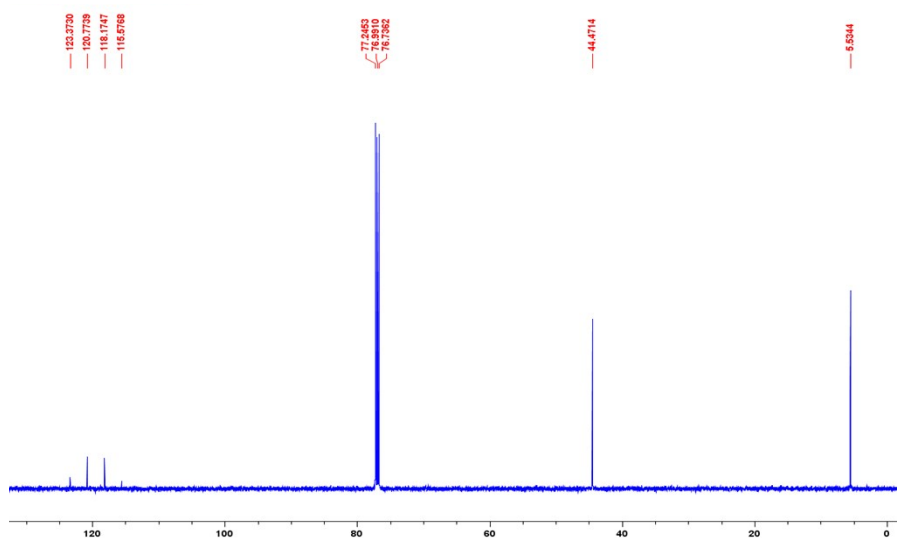
Fig. S2 ^{13}C NMR spectrum of ((trifluoromethyl)sulfonyl)ethane (FMES) in CDCl$_3$.
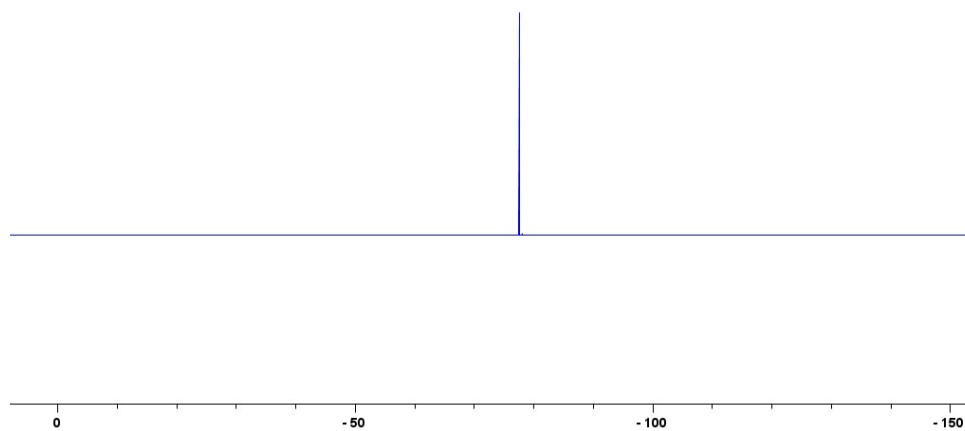

| 0 | - 50 | - 100 | - 150 |

Fig. S3 ^{19}F NMR spectrum of ((trifluoromethyl)sulfonyl)ethane (FMES) in CDCl$_3$.
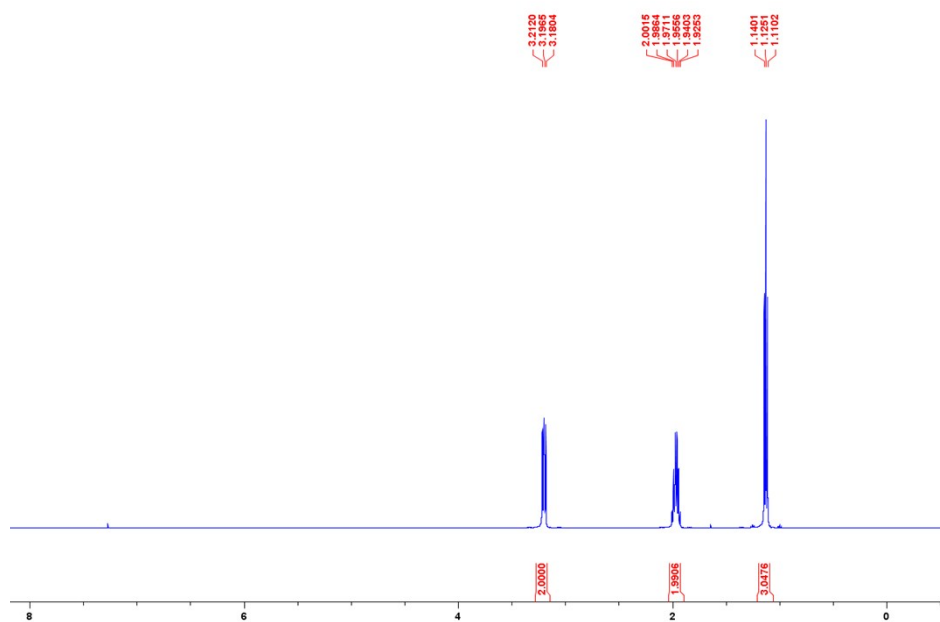
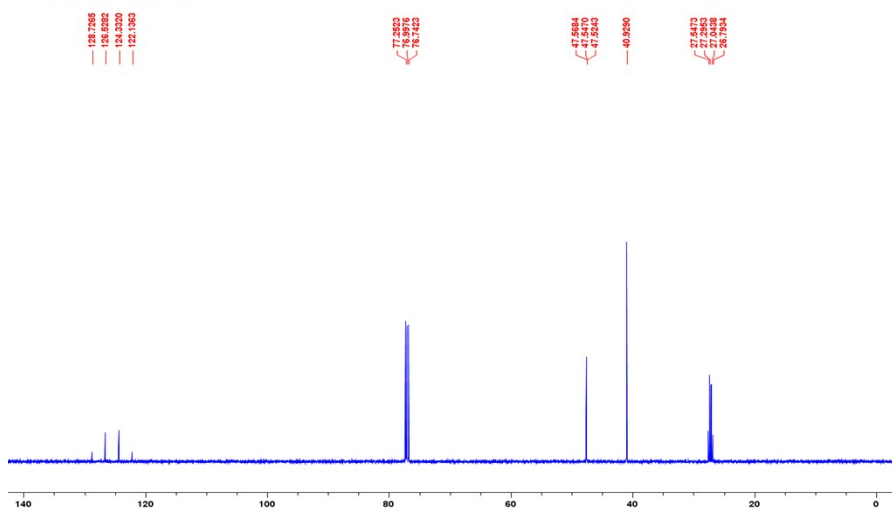**Fig. S4** ^{1}H NMR spectrum of 1-((trifluoromethyl)sulfonyl)propane (FMPS) in CDCl$_3$.

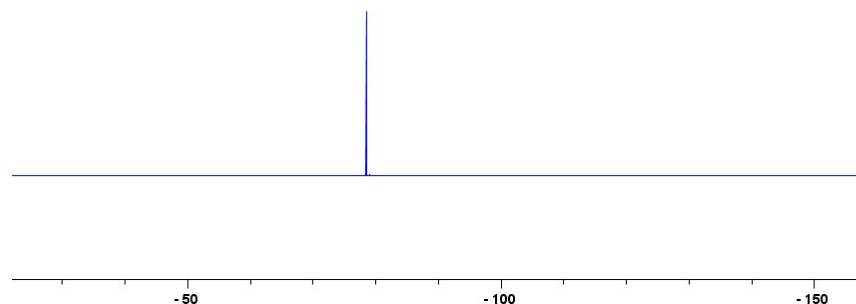**Fig. S5** ^{13}C NMR spectrum of 1-((trifluoromethyl)sulfonyl)propane (FMPS) in CDCl$_3$.

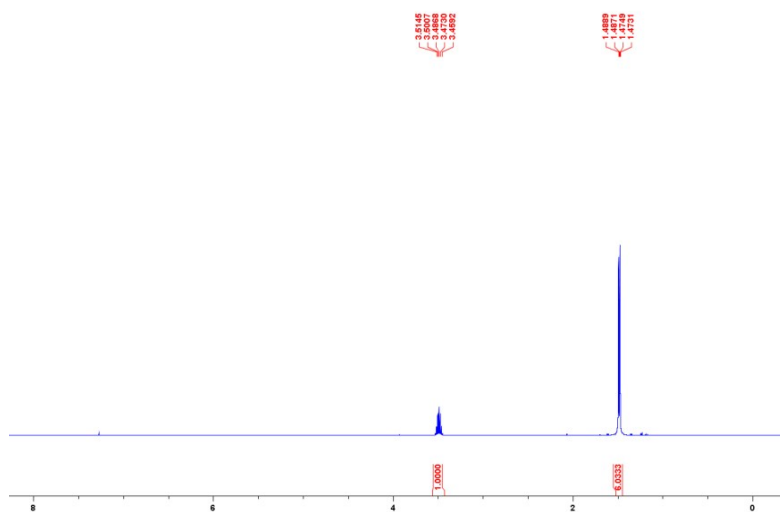**Fig. S6** ^{19}F NMR spectrum of 1-((trifluoromethyl)sulfonyl)propane (FMPS) in CDCl$_3$.

Fig. S7 ^{1}H NMR spectrum of 2-((trifluoromethyl)sulfonyl)propane (FMIS) in CDCl$_3$.
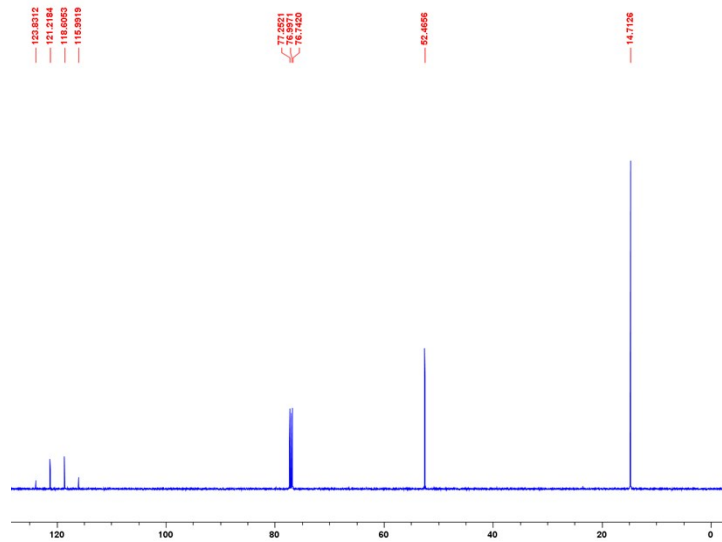
7

Fig. S8 ^{13}C NMR spectrum of 2-((trifluoromethyl)sulfonyl)propane (FMIS) in CDCl$_3$.
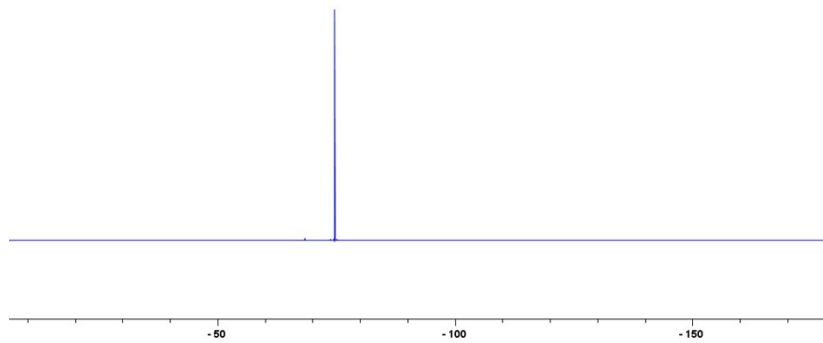

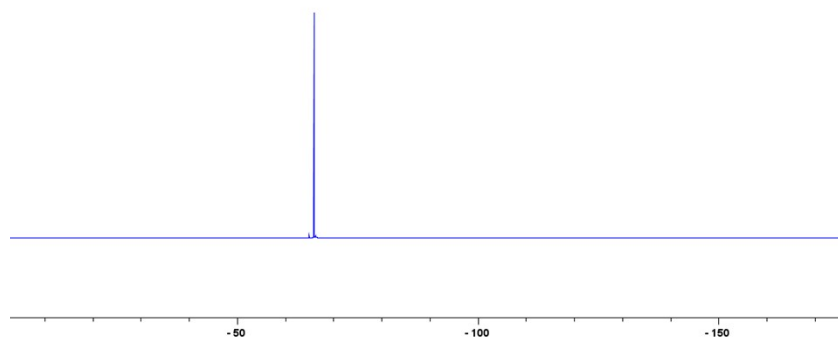**Fig. S9** ^{19}F NMR spectrum of 2-((trifluoromethyl)sulfonyl)propane (FMIS) in CDCl$_3$.
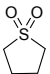
Fig. S10 ^{1}H NMR spectrum of 1,1,1-trifluoro-3-(methylsulfonyl)propane (FPMS) in CDCl$_3$.
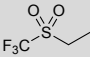

Fig. S11 ^{13}C NMR spectrum of 1,1,1-trifluoro-3-(methylsulfonyl)propane (FPMS) in CDCl$_3$.
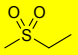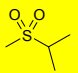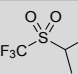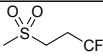
Fig. S12 ¹⁹F NMR spectrum of 1,1,1-trifluoro-3-(methylsulfonyl)propane (FPMS) in CDCl₃

Table S1 Selected Physical Properties of the Syntehsized Fluorosulfones. The Raws Are Color Coded to Facilitate the Comparison of EMS vs. FMES and MIS vs. FMIS

Sulfone	Chemical Structure	B.P. (ºC)	Contact Angle[a] (º)	Conductivity[b] (mS/cm)	Viscosity[c] (cP)
TMS		285 [d]	74	1.75	7.97
EMS		240 [d]	71	1.63	4.53
FMES		141	24	1.39	1.17
MIS		238 [e]	66	1.20	5.73
FMIS		150	28	0.99	1.20
FMPS		152	23	0.45	-

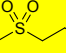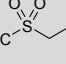[a]The contact angle between Celgard 2325 separator and a sulfone containing 0.5 M $LiPF_6$ at 20 ºC.
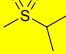[b]The conductivity of the solvent containing 0.5 M $LiPF_6$ at 20 ºC.
[c]The viscosity of neat solvent at 40 ºC.
[d]Ref. 22
[e]Ref. 23
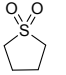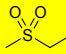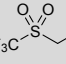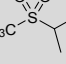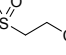
Sulfones	Chemical Structure	Oxidation Potential (V)	Reduction Potential (V)	HOMO Hartee	LUMO Hartee
TMS		6.22	0.85	-7.90	-0.37
EMS		6.34	0.80	-8.10	-0.41
FMES		6.76	1.43	-8.84	-0.62
MPS		6.29	0.79	-8.06	-0.36
FMPS		6.70	1.51	-8.78	-0.45
MIS		5.91	0.98	-7.93	-0.36
FMIS		6.28	1.68	-8.65	-0.46
FPMS		6.73	0.98	-8.55	-0.52

Density functional theory (DFT) calculations were performed using Gaussian 09 program suite. Oxidation and reduction potentials were calculated by optimizing the geometries of the species at the B3LYP/6-31G(p,d) level, followed by frequency calculations to determine gas-phase free energies. Solvation effects were taken into account by using a single-point B3LYP/6-31+G(p,d) polarized continuum model calculation. Finally, basis set effects were taken into account using a single-point B3LYP/6-311+G(3df,2p) calculation. From these results, the total free energy, electron affinities, HOMO and LUMO energies, and ionization potentials were calculated. These quantities were converted to standard electrode potentials as described elsewhere.

Fig. S13 Compatability of FMES/LiTSI electrolyte with graphite anode. (Li/graphite half cell charge and discharge voltage profiles).

S2. Fluorinated Sulfone Reduction Chemistry – Mechnistic Insight

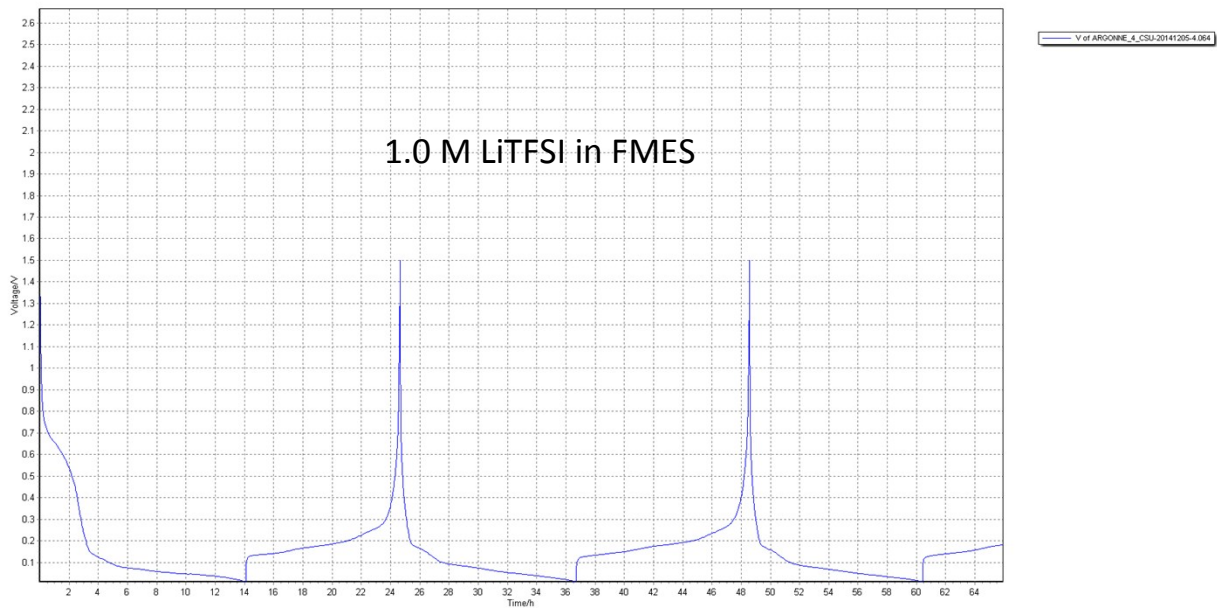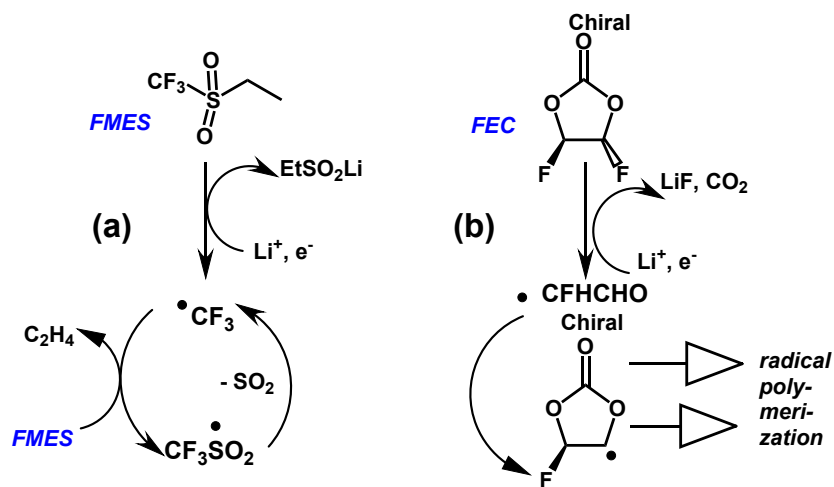**Fig. S14** Chemical reactions initiated by one-electron reduction of (a) FMES and (b) FEC.

For sulfones, desulfonylation by alkali metals, various reducing agents, and electrochemical reduction is a well-known reaction (Fig. S14a) that is used in preparative organic chemistry.[1-3]

$$Li^0 + RSO_2R' \rightarrow R\bullet + R'SO_2Li \qquad (S1)$$

From our DFT calculations, for EMS (R=Me and R'=Et, Fig. 1 in the manuscript), the elimination of methyl (ethyl) radical is exergonic by 1.58 eV and 1.68 eV, respectively, whereas for FMES (R=CF_3, R'=Et, Fig. 1), reaction S1 is even more exergonic (2.09 eV for trifulromethyl and 2.00 eV for ethyl elimination). In contrast, fluorine abstraction (reaction S2) is exergonic by only 0.72 eV

$$Li^0 + CF_3SO_2Et \rightarrow LiF + \bullet CF_2SO_2Et \qquad (S2)$$

That is, one electron reduction of the fluorinated sulfones favors C-S bond cleavage over C-F bond cleavage. This property has important implications for SEI formation, as illustrated in Fig. S13a. The released R$\bullet$ radicals (alkyl or trifluoromethyl) can abstract H from the solvent. Here another chemical peculiarity of the sulfones becomes important: the corresponding H loss radicals are unstable to C-S bond cleavage, therefore the overall reaction (X=CF_3 or CH_3)[4-7] is

$$R\bullet + XSO_2Et \rightarrow RH + XSO_2\bullet + C_2H_4\uparrow \qquad (S3)$$

While MeSO$_2\bullet$ radical is relatively stable,[5,8] $CF_3SO_2\bullet$ is weakly bound[8] and it readily dissociates

$$CF_3SO_2\bullet \rightarrow \bullet CF_3 + SO_2\uparrow \qquad (S4)$$

The released trifluoromethyl radical can react with another solvent molecule; so reactions S1 to S4 constitute a radical chain reaction causing the efficient solvent breakdown at the electrode surface. This chain terminates when two R$\bullet$ radicals recombine with each other. Since no radical polymerization appears to be possible in this solvent, the SEI does not have the outer polymer coating that is formed in the carbonate electrolytes,[9] which is generated through radical and anion polymerization of the partially reduced

solvent.[10-13] The resulting SEI is mainly consisting of lithium salts (like the ones formed in reaction S1 and Fig.S15a). As the cell goes through the lithiation/delithiation cycles, the resulting crystalline deposits (the inner mineral SEI layer) begin to crack and still more solvent decomposes, as there is no polymer overlayer (Fig.S15b) protecting these cracks and fissures in the deposit from direct exposure to the electrolyte. When FEC is added to this solvent, defluorination of this additive occurs at the surface,[14-18]

$$Li^0 + DFEC \rightarrow LiF + \cdot CFH_2CHO + CO_2 \quad \uparrow \qquad (S5)$$
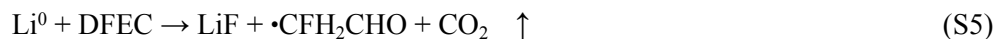
and the released vinoxyl radical (along with R$\cdot$ radicals released in reaction S1) can abstract H from DFEC molecules (Fig.S14b); this abstraction initiates radical reactions[12-14,19] leading to the formation of a cross-linked polymer, as explained in ref. 14. Thus, the presence of DFEC additive near the lithiated graphite electrode, can initiate the polymerization, and the inner mineral layer (of the completely reduced material)[20,21] is protected from above by an additional outer polymer coating that considerably stabilize the SEI. If the surface potential is insufficient to initiate solvent breakdown via reaction S1, such processes become irrelevant, and the addition of DFEC has little or no effect on the cell performance.
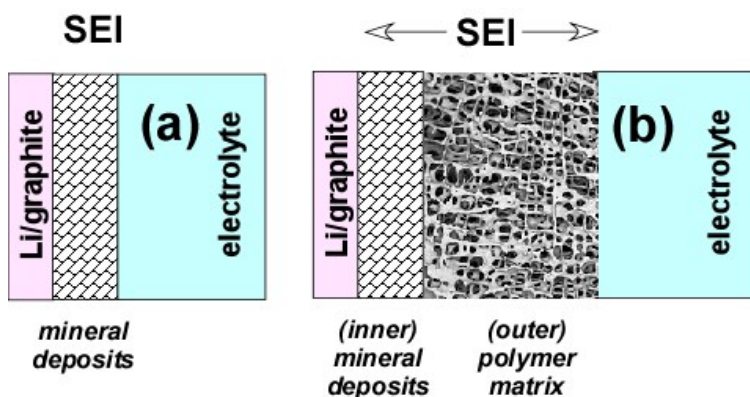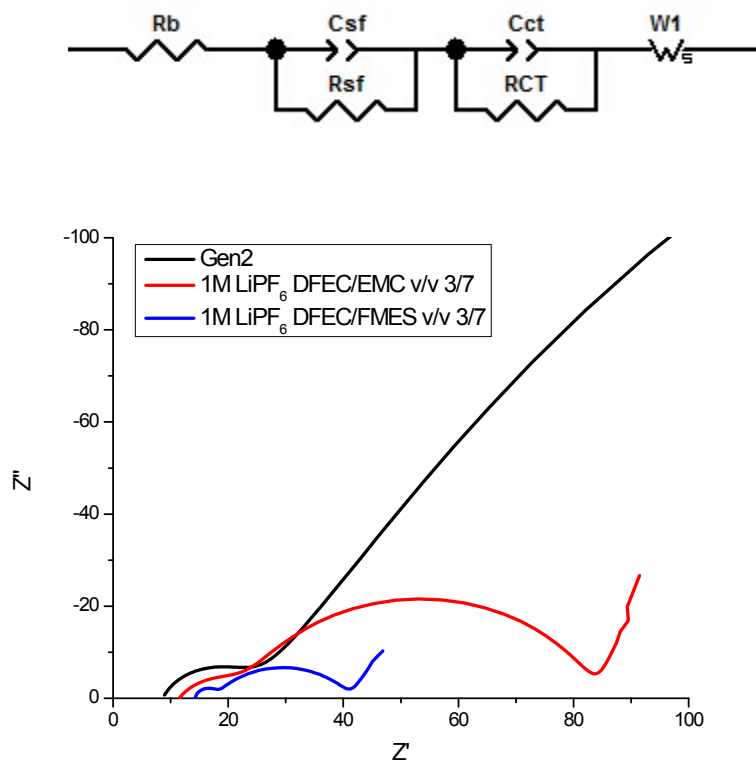

Fig. S15 Graphical representation of SEI morphology for (a) FMES and (b) FMES/DFEC.

15

Electrolyte	R_{bulk}	R_{SF}	R_{CT}
Gen2	8.6	14.1	191.7
1M LiPF$_6$ DFEC/EMC v/v 3/7	11.5	12.2	60.4
1M LiPF$_6$ DFEC/FMES v/v 3/7	14.3	3.3	23.7

Fig. S16 Electrochemical impdance spectra of the three electrolyte cells cycled for 500 cycles. (EIS measured at fully discahrged state).

S3. Electrode Preparation and Electrochemical Evalaution

S3.1 Electrode preparation

The cathode was made of 90 wt% NMC532, 5 wt% carbon black C45, and 5 wt% Solvay polyvinylidene fluoride (PVDF) 5130 binder coated on aluminum foil. The active material loading averaged 9.15 mgcm^{-2}. The graphite anode was made of 89.8 wt% Conoco Phillips CGP-A12, 4 wt% Super P-Li, 6 wt% Kureha PVDF 9300 binder, and 0.2 wt% oxalic acid coated on copper foil. The active material loading averaged 5.3 mgcm^{-2}. The effective diameters of cathode, anode and separator were 14 mm, 15 mm and 16 mm, respectively.

S.3.2 Electrochemical evaluation. Linear sweep voltammetry studies were performed using a Bio-Logic VMP3 electrochemical working station. The measurements were carried out in a three electrode Swagelok cell using Pt electrode (8 mm diameter) as working electrode and lithium as both counter (8 mm diameter)

and reference electrode (8 mm diameter) and glass fiber as the separator (10 mm diameter); the scan rate was 10 mV/s.

Galvanostatic charge-discharge cycling tests for NMC532/graphite coin cells (2032) were conducted on Maccor Electrochemical Analyzer (MIMSclient) with a cutoff voltages 3.0 V and 4.6 V. The effective electrode area was 1.6 cm^2. These cells were cycled at C/10 two times to form passivation layers; the subsequent trial involved 50 cycles at C/3 (0.67 mA). All electrochemical experiments were conducted at 25°C.

Supplementary References

1   J. Simonet, in *The Chemistry of Sulphones and Sulphoxides*, eds. S. Patai, Z. Rappoport and C. Stirling, Wiley-Interscience, Chichester, U. K., 1988, pp. 1001-1045.
2   F. Schoenebeck, J. A. Murphy, S.-z. Zhou, Y. Uenoyama, Y. Miclo and T. Tuttle, *J. Am. Chem. Soc.*, 2007, **129**, 13368-13369
3   L. Horner and H. Neumann, *Chem. Ber.*, 1965, **98**, 1715-1721.
4   F. Freeman and M. C. Keindl, *Sulfur Rep.*, 1985, **4**, 232-298.
5   B. C. Gilbert, R. O. C. Norman and R. C. Sealy, *J. Chem. Soc., Perkin Trans. 2*, 1975, 308-312.
6   B. C. Gilbert, R. O. C. Norman and R. C. Sealy, *J. Chem. Soc., Perkin Trans. 2*, 1975, 303-308.
7   P. M. Carton, B. C. Gilbert, H. A. H. Laue, R. O. C. Norman and R. C. Sealy, *J. Chem. Soc., Perkin Trans. 2*, 1975, 1245-1249.
8   D. Gonbeau, M. F. Guimon, S. Duplantier, J. Olliver and G. Pfister-Guillouzo, *Chem. Phys.*, 1989, **135**, 85-89.
9   A. von Cresce, S. M. Russell, D. R. Baker, K. J. Gaskell and K. Xu, *Nano Lett.*, 2014, **14**, 1405-1412.
10   K. Xu, *Chem. Rev.*, 2014, **114**, 11503-11618.
11   K. Xu, *Chem. Rev.*, 2004, **104**, 4303-4417.
12   I. A. Shkrob, Y. Zhu and D. P. Abraham, *J. Phys. Chem. C*, 2013, **117**, 19270-19279.
13   I. A. Shkrob, Y. Zhu and D. P. Abraham, *J. Phys. Chem. C*, 2013, **117**, 19255-19269.
14   I. A. Shkrob, J. F. Wishart and D. P. Abraham, *J. Phys. Chem. C*, 2015, **119**, 14954-14964.
15   K. Leung, S. B. Rempe, M. E. Foster, Y. Ma, J. M. Martinez del la Hoz, N. Sai and P. B. Balbuena, *J. Electrochem. Soc.*, 2014, **161**, A213-A221.
16   J. M. Martinez de la Hoz, K. Leung and P. B. Balbuena, *ACS Appl. Mater. Interfaces*, 2013, **5**, 13457-13465.
17   J. M. Martinez de la Hoz and P. B. Balbuena, *Phys. Chem. Chem. Phys.*, 2014, **16**, 17091-17098.
18   J. M. Martinez de la Hoz, F. A. Soto and P. B. Balbuena, *J. Phys. Chem. C*, 2015, **119**, 7060−7068.
19   F. A. Soto, Y. Ma, J. M. Martinez de la Hoz, J. M. Seminario and P. B. Balbuena, *Chem. Mater.*, 2015, **27**, 7990-8000.
20   X. Zhao, Q.-C. Zhuang, S.-D. Xu, Y.-X. Xu, Y.-L. Shi and X.-X. Zhang, *Int. J. Electrochem. Sci.*, 2015, **10**, 2515-2534.

21   C. Xu, F. Lindgren, B. Philippe, M. Gorgoi, F. Björefors, K. Edström and T. Gustafsson, *Chem. Mater.*, 2015, **27**, 2591-2599.